Environmental Science & Technology

pubs.acs.org/est

Article

Event-Based Atmospheric Precipitation Uncovers Significant Even and Odd Hg Isotope Anomalies Associated with the Circumpolar Vortex

Shengliu Yuan, Jiubin Chen, Holger Hintelmann,* Hongming Cai, Wei Yuan, Sheng He, Ke Zhang, Yuanyuan Zhang, and Yulong Liu

Cite This: *Environ. Sci. Technol.* 2022, 56, 12713−12722

Read Online

ACCESS | Metrics & More | Article Recommendations | Supporting Information

ABSTRACT: The determination of the mass-independent fractionation of even Hg isotopes (even-MIF, Δ^{200}Hg) in atmospheric samples adds another intriguing feature to the Hg isotope system. Despite our lack of sufficient experimental verification and the momentary absence of a valid mechanism to explain its occurrence, even-MIF could be instrumental in understanding the cycle and deposition of atmospheric Hg. In contrast to slightly positive Δ^{200}Hg values (<0.30‰) frequently observed in most atmospheric samples, large Δ^{200}Hg values (up to 1.24‰) determined in precipitation from Peterborough (Ontario, Canada) stand out and could provide valuable information for the origin of the even-MIF mystery. We now report a systematic analysis of high-resolution rainfall and snowfall samples collected in winter during cold weather at Peterborough, Canada. Dissolved and particulate Hg both displayed large variations of odd-MIF (from −0.93‰ to 2.02‰ for Δ^{199}Hg), which may result from long-range transportation, as the negative odd-MIF in particulate Hg is likely a result of long-distance transport of arctic atmospheric Hg(II). Dissolved Hg revealed significant even-MIF values (from 0.25‰ to 1.19‰ for Δ^{200}Hg) and a negative relationship between Δ^{200}Hg and Δ^{204}Hg, which provide further evidence for the previously proposed conceptual model of Δ^{200}Hg. Disconnected odd-MIF and even-MIF trends were detected in sequentially collected precipitation samples, which further suggests different sources or mechanisms for Δ^{199}Hg and Δ^{200}Hg. Particularly, the high Δ^{200}Hg values highlight the transport of stratospheric Hg through a polar vortex to the sampling region, stimulating further systematic investigation. The new Δ^{200}Hg data for particulate Hg add to existing information on atmospheric Hg(II) worldwide, suggesting a global distribution of Hg characterized by even-MIF in the atmosphere, and further constrain the model of atmospheric Hg deposition.

KEYWORDS: *atmospheric Hg, mass-independent fractionation (MIF), troposphere and stratosphere, wet deposition, polar vortex*

1. INTRODUCTION

Mercury (Hg) is an environmental neurotoxin of global concern. Hg bioaccumulates in organisms and biomagnifies in food webs, especially its organic form of monomethylmercury (MMHg, CH_3Hg^+), and may cause neurologic impairment to humans and other mammals worldwide, with a socioeconomic cost exceeding US $5 billion annually.[1−3] The Minamata Convention on Mercury was signed in 2013 and aimed at reducing global Hg pollution in the coming decades. The high Hg content in the troposphere and global mobility of gaseous elemental Hg (GEM), having an approximate atmospheric lifetime of 1 year, highlights the need for a better understanding of Hg transportation and fate in the atmosphere. Atmospheric Hg is subject to complex redox and physical processes,[4−6] and its deposition to terrestrial and marine ecosystems, including wet and dry deposition of particulate Hg (PHg) and reactive gaseous Hg (RGM), controls global Hg redistribution. Moreover, recent studies demonstrated that processes such as atmospheric Hg depletion events (AMDEs) and vegetation uptake of gaseous Hg(0) in pan-Arctic regions would be the driving force behind critical processes.[5,7] Currently, the absence of direct, long-term observations of Hg in the upper atmosphere makes it difficult to constrain atmospheric Hg dynamics and relative deposition fluxes. Precipitation likely scavenges Hg(II) (mainly RGM and PHg) present in clouds and below clouds and delivers it to surface ecosystems.[8,9] Thus, the Hg in precipitation presumably integrates the chemistry of Hg present in the upper atmosphere (or free atmosphere) and the atmospheric boundary layer (ABL) and could provide insights into the deposition of atmospheric Hg and relative ecological effects.

The Hg isotope approach has been utilized to characterize the transportation and transformation of atmospheric Hg: e.g.,

Received: April 19, 2022
Revised: August 1, 2022
Accepted: August 7, 2022
Published: August 18, 2022

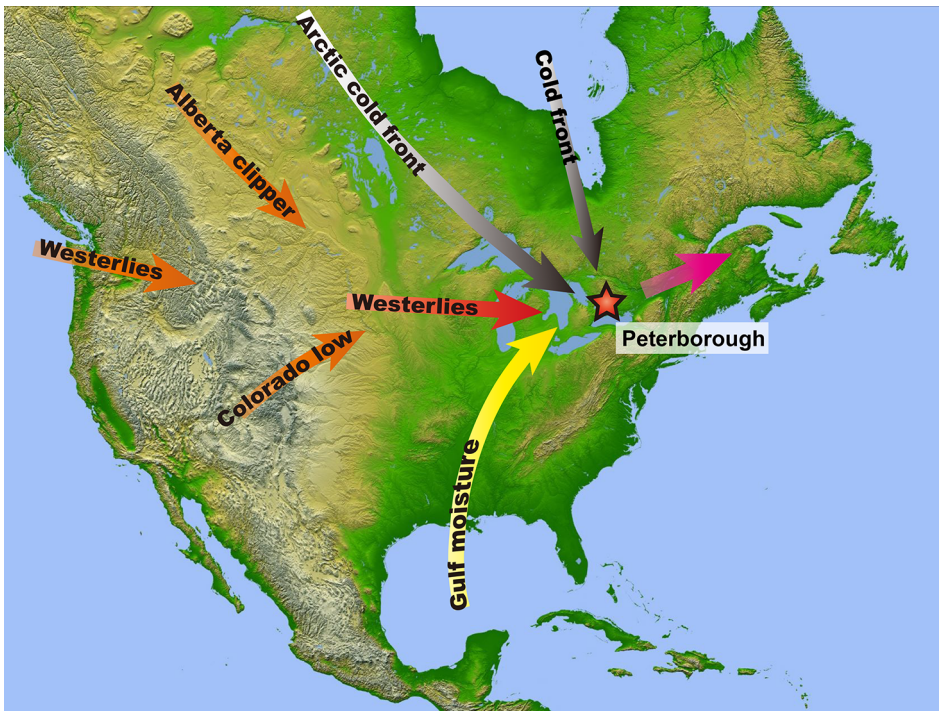

Figure 1. Study site and meteorological features of major regional events.

by determining mass-dependent fractionation (MDF, represented by δ^{202}Hg), mass-independent fractionation (MIF) of odd isotopes (odd-MIF, reported as Δ^{199}Hg and Δ^{201}Hg) and even isotopes (even-MIF, reported as Δ^{200}Hg and Δ^{204}Hg).[10−13] Almost all atmospheric processes exhibit MDF of Hg isotopes, including but not limited to the chemical processes and the physical processes of adsorption and desorption and diffusion, volatilization, and dissolution to droplets.[5,14−19] Due to the universal existence of photoreduction, odd-MIF was observed in all samples related to the atmosphere.[20,21] Odd-MIF of atmospheric Hg(II) was significantly different between aerosol and precipitation, suggesting a difference between *in situ* emissions and long-range transport of Hg.[11,22−24] Complementary even-MIF values found in total gaseous mercury (TGM) and precipitation,[5,11,12,21,25−27] combined with atmospheric back trajectory analysis, suggested that Δ^{200}Hg was exclusively generated by photochemical oxidation in the tropopause and was therefore considered as a conservative tracer for atmospheric Hg deposition.[11,18,28]

Nevertheless, the fractionation mechanism triggering even-Hg isotope anomalies is not well understood. A ^{204}Hg anomaly emerged in more recent studies, and it was suggested that the apparent ratio of Δ^{200}Hg to Δ^{204}Hg (∼−0.5) may provide insights into even-Hg isotope fractionation mechanisms.[21,29] The largest magnitude of even-MIF was observed in compact fluorescent light bulbs, where a self-shielding effect was proposed to explain the relationship between Δ^{200}Hg and Δ^{204}Hg.[30] However, it needs to be further explored if this may also be a promising explanation for naturally occurring even-MIF. Especially the large magnitude of Δ^{200}Hg (up to 1.24‰) observed in winter precipitation[11] may serve as a starting point to explore the true mechanism of the even isotope anomaly. However, many studies showed absolute values of less than 0.30‰ for Δ^{200}Hg,[11,21,31] including snow samples from the Great Lakes region impacted by the Arctic, highlighting the necessity of a more in depth investigation of precipitation Hg in this unique place.

Only a few recent studies reported similar Δ^{200}Hg values in either dissolved or particulate precipitation phases. However, some studies reported lower odd-MIF in particulates relative to dissolved Hg,[22,23,32] which promotes a further investigation of Hg isotopes in both phases. Moreover, global warming and abnormal distribution of precipitation may result in more uncertainties of Hg wet deposition.[33−35] Based on the above, a systematic survey and analysis of Hg isotopic composition of dissolved and particulate Hg in atmospheric precipitation was conducted from Winter 2020 to Spring 2021 in Peterborough, Canada, to confirm abnormal even-MIF data. Sequential samples were also collected during single precipitation events characterizing key parameters potentially responsible for the physiochemical transformation of Hg (and its isotopes) before and during the deposition, to eventually reveal the possible cause of the even isotope anomaly.

2. SAMPLE COLLECTION

All samples were collected in Inverlea Park (44.32°N, 78.32°W) at the north end of the City of Peterborough (Ontario, Canada; Figure 1). Peterborough is situated in Central Ontario within the Kawartha Lakes region and lies in the St. Lawrence Lowlands ecoregion, just south of the Canadian Shield and approximately 35 km north of Lake Ontario. The city is situated on a series of rapids in the Otonabee River and has a humid continental climate with four distinct seasons. Its climate can be quite unpredictable and varies greatly due to topography changes in elevation. There are no Hg sources or any known major Hg point sources in this region.[11,32]

Sampling was performed in cold months from November 2020 to March 2021 (Table S1). The precipitation samples (rain, snow, or mixture) were collected as soon as possible after the precipitation event started. Rainwater or snow was

https://doi.org/10.1021/acs.est.2c02613
Environ. Sci. Technol. 2022, 56, 12713−12722

sequentially collected over time during 13 precipitation events. Ten one-event samples were collected over the entire duration of a single precipitation event (Table S1). A homemade tilted "V" type PE sheet (surface area of ~1.6 m^2) was used to collect and channel rain samples into a precleaned 10 L glass jar wrapped with aluminum foil. All surfaces of the sampler system were covered with new PE film and precleaned by rinsing with Milli-Q water just before collection, contributing a blank of less than 26 pg (n = 7). The water was transferred into PTFE bottles or 10 L glass jars (soaked and cleaned first with 1% BrCl in 10% HNO_3 and then rinsed with Milli-Q water before use), packed in black bags, and stored at 4 °C. The snow samples were collected from the sheet and stored frozen at −20 °C using new PE bags (Nasco, USA) packed in black bags, which were precleaned by rinsing with Milli-Q water, showing blanks of <20 pg (n = 7). Finally, snow samples were melted in the dark after removal of outer snow layers and filtered using 0.45 μm cellulose membranes. The obtained filtrates and particles were processed for Hg isotope ratio measurements as described elsewhere.[11,23] Details of the analytical procedure are provided in the Supporting Information.

3. RESULTS AND DISCUSSION

3.1. Variations of Hg Concentrations and Isotopic Compositions. In comparison to the precipitation collected in Peterborough in 2010,[11] the concentrations of dissolved Hg concentrations were slightly lower (2.80 ± 3.91 ng/L, n = 53) in 2021 compared to the same period in 2010 (3.02 ± 2.12 ng/L, n = 8). If the samples of the last two events were excluded, the average concentrations decreased even further (1.75 ± 0.94 ng/L, n = 44). Similar observations were made for the Great Lakes region. Snow samples (total Hg = 1.82 ± 1.15 ng/L, n = 8) also revealed a much lower Hg concentrations than in rain samples collected 10 years ago (total Hg = 14.84 ± 8.96 ng/L, n = 17).[31,32,36]

Isotopically, all samples presented large isotope fractionation. Relative to 10 years ago (δ^{202}Hg, −0.91 ± 0.42 ‰, n = 8; Δ^{199}Hg, 0.38 ± 0.39‰, n = 8), the dissolved Hg was characterized by a more positive δ^{202}Hg ($\delta^{202}Hg_D$, −0.16 ± 0.41‰, n = 53) and Δ^{199}Hg ($\Delta^{199}Hg_D$, 0.94 ± 0.43‰, n = 53). All dissolved Hg showed relatively highly positive Δ^{200}Hg ($\Delta^{200}Hg_D$, from 0.25‰ to 1.19‰ with an average of 0.48 ± 0.20‰), which was slightly lower than that measured in samples of the same period 10 years ago (0.79 ± 0.39 ng/L, n = 8); however, the values were still much higher than those for other precipitation samples reported. All samples, except for S-12 (0.04‰), displayed negative particulate δ^{202}Hg ($\delta^{202}Hg_P$, −0.65 ± 0.31 ng/L, n = 53). Almost all particulate Hg samples showed positive Δ^{199}Hg ($\Delta^{199}Hg_P$, 0.42 ± 0.41‰, n = 53), except for two samples (S-12 and S-24). Likewise, a positive Δ^{200}Hg ($\Delta^{200}Hg_P$) was generally found in particulate samples, except for S-12.

3.2. Significant Variations of odd-MIF. In this study, all precipitation samples were collected during the cold season, from November 2020 to March 2021. Dissolved Hg displayed positive and significant odd-MIF (Figure 4). Compared to samples collected during the same period 10 years ago, the more positive δ^{202}Hg and Δ^{199}Hg may suggest a difference in sources or a change in source contributions. Due to high coal consumption and combustion in the winter, the local/regional Hg emission should be generally higher in the winter than in the summer and result in higher Hg concentrations. Chen et al.[11] pointed out that the city of Peterborough is located within the Kawartha tourist region and local Hg contributions are limited. Hence, Hg in precipitation should be mainly derived from moderate distance transport. Combining meteorological data and back trajectories of air masses, the anthropogenic Hg emissions from the greater Toronto area and even the Great Lakes region (southern contribution) were still considered to be the main contributions. However, lower present-day concentrations in precipitation compared to 10 years ago may suggest declining emission of anthropogenic Hg regionally and would point to the effectiveness of Hg emission reductions during the past decade.[37] A similar decline of Hg concentration was also found in snow samples from the Great Lakes region.[31,32,36] Moreover, several samples with higher Hg concentrations showed lower Δ^{199}Hg, and most samples displayed lower concentrations and higher Δ^{199}Hg compared to 2010 (Figure S2), further supporting a decline in anthropogenic emissions (close to zero Δ^{199}Hg).

Previous event precipitation samples and sequential samples during the same event indicated that *in situ* physical and chemical atmospheric processes result in little MDF and MIF.[23,24,28,38] The higher δ^{202}Hg and Δ^{199}Hg found in this study may suggest a higher proportion of Hg from long-range transport (Figure 4).[23,28,38] Chen et al.[11] had reported that Hg originating from the center/western continent, northern Canada, and even the pan-Arctic could contribute to Hg in Peterborough precipitation. Current air parcel back trajectories (Figures S7 and S8), as well as measured moderate values of δ^{18}O (~−10‰) and d-excess (~15‰) would indeed support the idea that air masses passed through the continent.[34] Likewise, low δ^{18}O (<−16‰) and high d-excess (>20‰) suggest that air masses originated from cold environments (such as the pan-Arctic region) (Figures S7 and S8). Since these regions consist mainly of boreal forest or tundra with limited human activity, anthropogenic Hg emissions are likely negligible and would therefore not result in high positive Δ^{199}Hg values, due to vegetation−air exchange.[39] Hence, the atmospheric Hg arriving through long-range transport must have been subject to a relatively higher intensity of photoreduction, thus resulting in the observed high δ^{202}Hg and Δ^{199}Hg values. Previous precipitation samples collected in sequence further revealed the contribution of different dominant sources.[23] This level of detail is obscured in composite samples from one or multiple events.[23,38] For example, the two successive samples (S-20, S-21) of E-11 show a large difference (0.93‰) for $\Delta^{199}Hg_D$, which suggests that a second fraction of Hg with a relatively high Δ^{199}Hg value (S-21) arrived after long-range transport as well as other events in this study (Table S1).

Likewise, particulate Hg was also characterized by a large $\Delta^{199}Hg_P$ value (0.42 ± 0.31‰, n = 52), with individual values of up to 1.20‰ (RS4). Though generally lower than $\Delta^{199}Hg_D$ in this study, the $\Delta^{199}Hg_P$ values were higher than those found for total Hg in precipitation across North America.[31,32,36,40,41] The observed $\Delta^{199}Hg/\Delta^{201}Hg$ ratio of 0.985 ± 0.048 (Figure S1A) indicates likely photoreduction of Hg(II) as the origin of positive Δ^{199}Hg.[21] In fact, the local/regional Hg emissions (including geological aerosol) with a Δ^{199}Hg value of ~0‰ would be mainly present in ABL and deposition from below-cloud scavenging. These contributions are expected to be more important for particulate Hg in precipitation, resulting in lower $\Delta^{199}Hg_P$ in comparison to $\Delta^{199}Hg_D$.[23] As a result, the high $\Delta^{199}Hg_P$ is proposed to originate from long-range transport,

https://doi.org/10.1021/acs.est.2c02613
Environ. Sci. Technol. 2022, 56, 12713−12722

undergoing intense photoreduction.[11,23,28] This process itself would mainly occur after in-cloud scavenging. The limited literature on the photoreduction of particulate Hg(II) suggests that negative odd-MIF values are a result of aerosol phase reactions, while positive odd-MIF was observed in aqueous-phase reactions of soot Hg.[42] However, the magnitude of aerosol-phase Hg(II) photoreduction was limited, the photoreduction of aerosol Hg(II) in aqueous environment was supposed to be the dominant factor.[42] Consequently, the wet deposition of particulate Hg is likely a significant source of positive Δ^{199}Hg measured in western Great Lakes sediments.[43]

However, the low $\Delta^{199}Hg_D$ value found in S-20 (0.11‰) and even negative $\Delta^{199}Hg_P$ values (−0.93‰ and −0.52‰, respectively) of two samples (S12 and S24) may indicate additional Hg source(s). In the winter, the southward cold air mass originating from the Arctic region cannot be ignored, as it may transport Arctic atmospheric Hg(II) to Peterborough.[11] Previous studies pointed out that almost no odd-MIF is generated during the GEM photo-oxidation by bromine or BrO in polar regions,[5,25,44] and the initial isotopic signature in snow corresponded with a similar negative Δ^{199}Hg value in the surrounding atmospheric Hg(0).[32,45] After exposure to sunlight, Hg(II) in snow is possibly photoreduced by halogens and the residual Hg(II) generally displayed a more negative Δ^{199}Hg value,[5,46] as low as −3.45‰ in high Arctic fresh snow.[25] Similarly, the more negative Δ^{199}Hg values were also detected in aerosol samples from the high Arctic.[25] Subsequently, atmospheric Hg(II) with a negative Δ^{199}Hg value was likely transported southward by the cold air mass in winter, especially during the polar vortex in the low troposphere (Figures S7 and S8), resulting in the relatively low $\Delta^{199}Hg_D$ values in S12 and S24. For both of those samples, the dissolved Hg presented higher δ^{202}Hg and Δ^{199}Hg values. For S12, the differences are 0.25‰ and 1.06‰ for δ^{202}Hg and Δ^{199}Hg, respectively. The ratio (above 1.06‰/0.25‰) of differences was similar to aqueous Hg(II) photoreduction derived from Zheng and Hintelmann.[20] We therefore propose that Arctic Hg(II) was the dominant source to both Hg_D and Hg_P of lower or even negative Δ^{199}Hg. During the long-range transport of Arctic Hg(II), the photoreduction of aqueous Hg(II) could likely introduce the high δ^{202}Hg and Δ^{199}Hg values,[11,20] which further supports the contribution of Arctic Hg(II) by long-range transport.

3.3. Verification of Significant Even-Hg Isotope Anomalies. Gratz et al.[31] and Chen et al.[11] reported a significant even-Hg isotope anomaly (Δ^{200}Hg) in atmospheric precipitation. A conceptual model was established as a result of atmospheric Hg(II) oxidation in the tropopause to explain the high Δ^{200}Hg values especially in the winter, based on the relationship between Δ^{200}Hg and Na concentrations and the back trajectories of air masses.[11] However, most global precipitation samples (Figure 5, excluding polar regions) present only slightly positive Δ^{200}Hg values, mostly less than 0.30‰. The Δ^{200}Hg value of 1.24‰ found in snowfall from Peterborough was still one of the highest values reported in natural samples.[21,30] A decade later, winter precipitation was again collected here in Peterborough and indeed confirmed high positive Δ^{200}Hg values (up to 1.19‰ for S20) for the region (Figure 2).[21] In addition, the positive relationship between Δ^{200}Hg and average temperature during precipitation periods (Figure S3), coupled with the air mass back trajectories (Figures S7 and S8), further supports the model of its upper atmosphere origin developed by Chen et al. Here, all samples

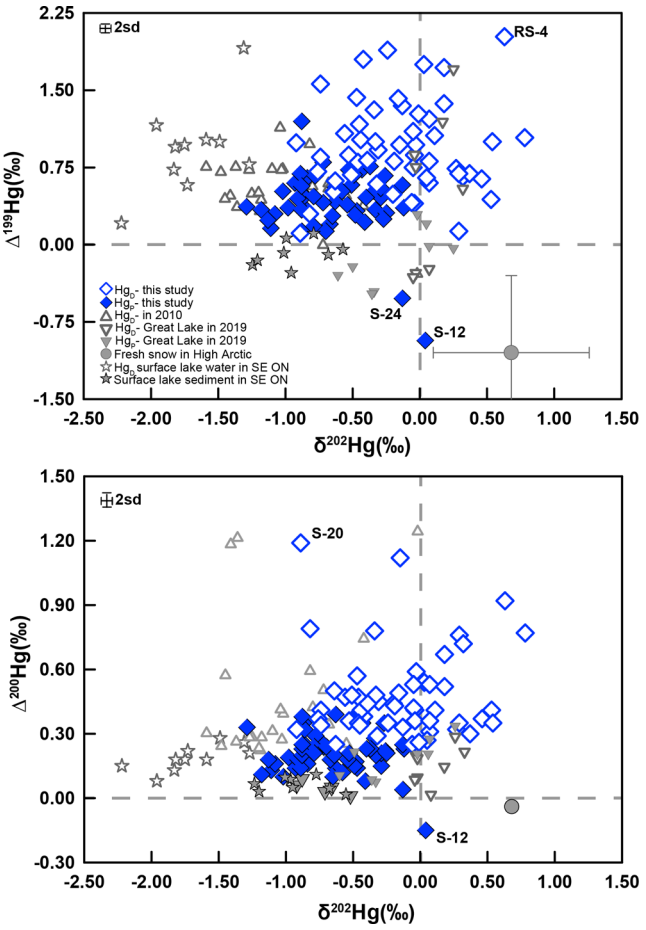

Figure 2. Mass-dependent and mass-independent Hg isotope compositions of dissolved and particulate phases in atmospheric precipitation from Peterborough, ON, Canada. Other data were reported previously.[11,13,25,32,43]

displayed significant Δ^{204}Hg values, ranging from −1.97‰ (Hg_D in S20) to −0.17‰ (Hg_P in RS3), with averages of −0.86 ± 0.39‰ (n = 53) and −0.42 ± 0.18‰ (n = 52) for Hg_D and Hg_P, respectively. The regression of Δ^{200}Hg against Δ^{204}Hg yielded slopes of −0.47 and −0.37 for Hg_D and Hg_P, respectively (Figure S1B), which was consistent with previous observations.[21] It is worth noting that limitations of ion beam collector designs of MC-ICP-MS, in combination with small isotopic signals in natural samples, often prevented the accurate determination of Δ^{204}Hg in previous studies. As we always monitored the signal at m/z = 206 to ensure that neither HgH_2 nor Pb were present at a significant level, we are confident that the measured Δ^{200}Hg and Δ^{204}Hg anomalies are true features of the samples and were not caused by interferences during MC-ICP-MS analyses.[21]

Low $\Delta^{200}Hg_D$ values of ~0.30‰ were also characterized by the samples of E13 and E14 and were similar to those of most samples measured elsewhere.[23] E13 and E14 had higher Hg concentrations, and the back trajectories of air mass (Figures S7 and S8) suggested an influence of local/regional emissions of Hg. Meanwhile, most of the particulate Hg displayed lower but positive Δ^{200}Hg values (0.21 ± 0.10‰, n = 52), consistent with other studies measuring particulate Hg in precipitation, where Hg presented both contributions of local emissions and long-range transport.[11,22,23,38] However, the $\Delta^{200}Hg_P$ value of S-12 was negative (−0.15‰). As discussed previously for the

https://doi.org/10.1021/acs.est.2c02613
Environ. Sci. Technol. 2022, 56, 12713−12722

formation of negative $\Delta^{199}Hg_P$, this would suggest a contribution of atmospheric Hg(II) from the Arctic, where Hg was exposed to specific photoreduction.[5,25,46] Nevertheless, there is almost no even-MIF during these processes, and the atmospheric Hg(II) (including snow and aerosol) in Arctic samples displays negative $\Delta^{200}Hg$ values similar to those of GEM.[5,25,46] Since no even-MIF was reported for photoreduction processes, it would suggest that particulate Hg retains the isotope information on the source, even after long-range transport to Peterborough (Figures S7 and S8). During this snow event, the similarity of $\delta^{18}O$ and d-excess as well the back trajectories of air masses (Figures S7 and S8) suggest consistent sources of Hg throughout the event. The proportion of Arctic Hg(II) at the start of the event could be lower, due to scavenging of local atmospheric Hg, leading to also lower concentrations later on, when Hg in precipitation is dominated by Hg from long-range transport, as reported by Yuan et al. Hg_P showed a decrease in $\Delta^{199}Hg$ and $\Delta^{200}Hg$. The samples of S-12 even displayed negative $\Delta^{199}Hg$ and $\Delta^{200}Hg$ values, close to values found for atmospheric Hg(II) in the Arctic,[5,25,46] which may suggest the conservative behavior of particulate Hg in snow as well.

3.4. Sequential Samples during Polar Vortex. The sequential sampling of single-precipitation events in previous studies indicated that a change of dominant sources during the event could result in large variations of MDF and odd-MIF.[23] Even-MIF did not change, as both phases presented a low positive $\Delta^{200}Hg$ value of less than 0.30‰,[23,32,47] which could make sequential sampling of events a powerful strategy to explore the variation of sources during precipitation. In this study, the sequential sampling of 14 events was conducted with time; the high $\Delta^{200}Hg$ and its large variation may help to investigate the cause of even-MIF.

The five samples collected on February 15−22, 2021, when the stratospheric polar vortex struck North America, showed the largest variations of $\Delta^{199}Hg$ and $\Delta^{200}Hg$ (Figure 3). During this period, the atmospheric circulation over the continent was relatively regular. The progressively increasing $\delta^{18}O$ and d-excess indicated a decreasing proportion of Gulf moisture together with a increasing proportion of Arctic cold air mass (Figure 3B).[34] This was further supported by back trajectories of air masses (Figure S8). The last two samples of this period showed disconnected trends for both $\Delta^{199}Hg$ and $\Delta^{200}Hg$ (Figure 3C) in sequential samples. In particular, the first sample (S-20) had the highest $\Delta^{200}Hg_D$ value (1.19‰) and the lowest $\Delta^{199}Hg_D$ value (0.11‰), which may suggest contribution of different sources for $\Delta^{199}Hg$ and $\Delta^{200}Hg$.[23,32] Air mass back trajectories suggest that an upper atmosphere air mass descends over the Peterborough region and is then carried northward by warm moisture (Figure S8). Due to the high percentage of atmospheric Hg(II) from the upper atmosphere at this stage, both particulate and dissolved Hg in S-20 displayed higher $\Delta^{200}Hg$ values. However, concurrent Hg scavenging during the precipitation event decreases the proportion of Hg(II) from the upper atmosphere and the last two samples now presented lower $\Delta^{200}Hg$ values. The uniform and lower $\Delta^{200}Hg_P$ values (0.08−0.33‰) of these samples also indicated low contributions of Hg from the upper atmosphere. Hg from Gulf moisture and local emissions may also contribute to the lower $\Delta^{199}Hg$ value of S-20. In addition, Arctic Hg(II) with a negative $\Delta^{199}Hg$ value was not entirely excluded.[5,25,46] The lower $\Delta^{199}Hg$ value in S-24, particularly the negative $\Delta^{199}Hg_P$ value, suggests a probable contribution of

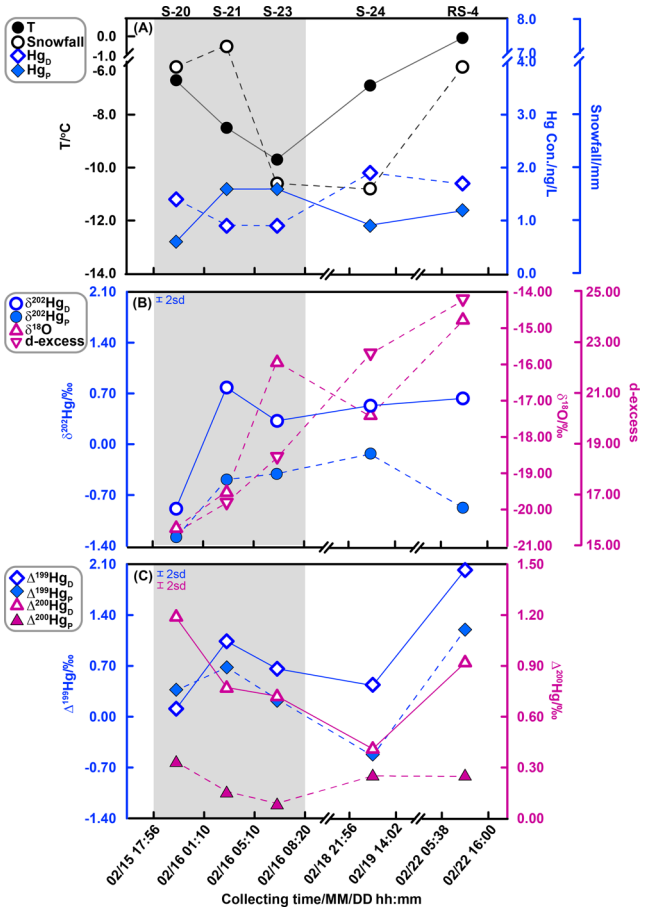

Figure 3. Temperature, snowfall, $\delta^{18}O$, d-excess, Hg concentrations, and isotope data in snow samples collected on February 15−22, 2021, when the polar vortex struck the Southern Plains in North America. Samples located in the gray aera were collected sequentially during a single snow event; the others were single-event samples.

Arctic Hg(II) with negative $\Delta^{199}Hg$ value. In conclusion, the inconsistent trends of $\Delta^{199}Hg$ and $\Delta^{200}Hg$ further support, in addition to the upper atmospheric origin of Hg(II),[11,12] a mixed contribution of atmospheric Hg(II) through the Arctic vortex in both the stratosphere and troposphere.

The second highly positive $\Delta^{200}Hg$ (1.12‰, S-11) event was observed in E7 midway in a polar vortex (Figure 4). The uniform $\delta^{18}O$, d-excess, and back trajectories of air masses (Figure S7) indicated that the atmospheric circulation over the continent was relatively stable (Figure 4B). Due to the movement of air masses, the highest $\Delta^{199}Hg$ and $\Delta^{200}Hg$ values for dissolved Hg were characterized at this midpoint (S-11 in Figure 4C) and a similar peak was found in $\Delta^{200}Hg_P$. Toward the end of the event, $\Delta^{199}Hg$ and $\Delta^{200}Hg$ both presented low values (S-12). However, $\Delta^{199}Hg_P$ and $\Delta^{200}Hg_P$ displayed negative values of −0.93‰ and −0.15‰, respectively, suggesting a high contribution of atmospheric Hg(II) from the Arctic. The positive $\delta^{202}Hg$ value was also indicative of background Hg (Arctic Hg(II)),[5,25,46] which was consistent with a contribution of arctic atmospheric Hg(II), resulting in the low $\Delta^{199}Hg$ and $\Delta^{200}Hg$ values of S-23 in the polar vortex event. Thus, the two events could indicate that atmospheric Hg(II) originating from the Arctic stratosphere and troposphere contributes to the high $\Delta^{200}Hg$ and low $\Delta^{199}Hg$ values in precipitation, respectively.

https://doi.org/10.1021/acs.est.2c02613
Environ. Sci. Technol. 2022, 56, 12713−12722

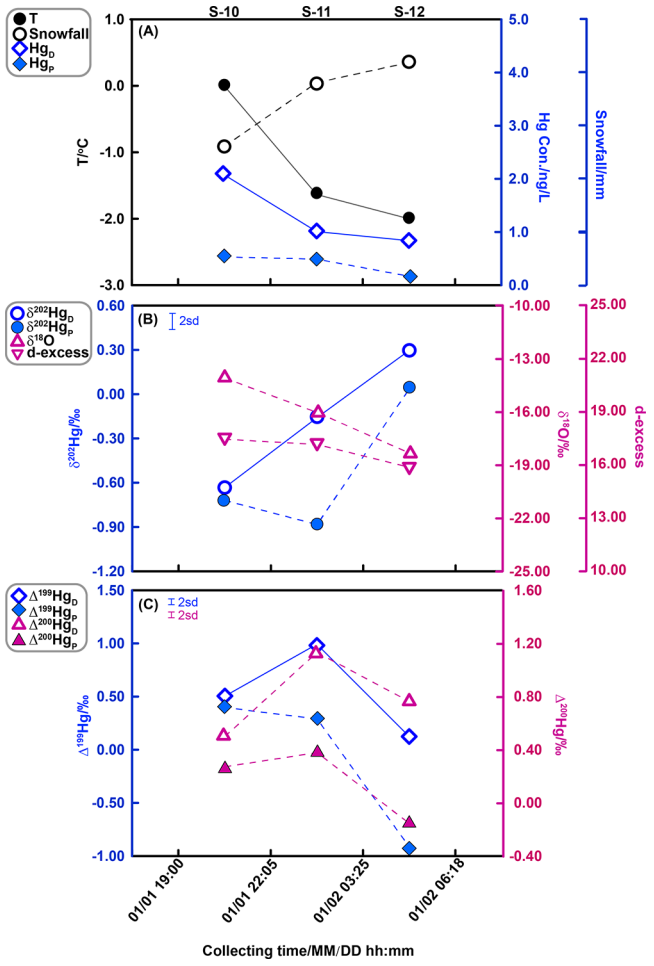

Figure 4. Tempertaure, snowfall, $\delta^{18}O$, d-excess, Hg concentrations, and isotope data in sequential snow samples collected on January 1−2, 2021, when the polar vortex struck North America.

This further suggests that the descent of two air masses from the stratosphere and troposphere occurred almost concurrently during the polar vortex but that their pathways of deposition and Hg transport were out of sync. The disruption of the polar vortex caused the polar stratospheric jet stream to become "wavier", stretch out of shape, and slide southward off the pole. In combination with other weather patterns, it created favorable conditions for the stratospheric intrusion. In the last decades, global warming has intensified as much as two-fold in the Arctic.[48] Even in Peterborough, the average temperature in winter (December, January, and February) mirrored the increasing tendency (Figure S6). Though highly positive Δ^{200}Hg values were measured for atmospheric precipitation in this study, overall, the average values were lower than those found 10 years ago (Figure 4B). As such, the negative relationship between Δ^{200}Hg and temperature (Figure S3) may suggest that long-term monitoring of Δ^{200}Hg in atmospheric precipitation could help to find the answer for the true mechanisms triggering even-MIF beyond the empirical relationship between Δ^{200}Hg and temperature and could even contribute to estimating the severity of regional/global climate change, as proposed by Chen et al.

3.5. Global Distribution of Even-MIF in Atmosphere.

Figure 5 summarizes the Δ^{200}Hg values of the global atmospheric precipitation. All samples showed positive values, mostly below 0.30‰, with the exception of high values in Peterborough and negative values the in pan-Arctic region. So far, the highest Δ^{200}Hg values were previously detected mostly in winter samples from the Peterborough region.[11] Peterborough lies in the St. Lawrence Lowlands ecoregion, just south of the Canadian Shield and has a humid continental climate. Here, the Arctic air interacts with the warm Gulf moist air mass, causing unstable weather conditions. In winter, the jet stream in the upper troposphere and stratosphere weakens and the stratospheric polar vortex occasionally intrudes southward and downward, transporting atmospheric Hg(II) from the upper atmosphere downward to the troposphere. The warm air mass could coerce the atmospheric Hg(II) from the upper atmosphere northward (Figures S7 and S8), where it meets a cold front and forms rain or snow. Meanwhile, the perennial westerlies prevailing in the midlatitudes could propel bands of precipitation eastward. Moreover, the above air masses may be restrained over the Great Plains by the Rocky Mountains (in the western region), Appalachian Mountains (in the eastern region), and the Canadian Shield (in the northern region), and then move northeastward. Thus, the frontal precipitation could scavenge Hg(II) from stratospheric intrusion and result in the highly positive Δ^{200}Hg values observed in snow or rainfall.

In this study, samples collected in spring (March) mostly displayed Δ^{200}Hg values that were close to those found in other atmospheric precipitation worldwide (Figure 5). This also indicated that the stratosphere intrusion barely occurs outside of the winter season. Most precipitation samples collected in midaltitude regions during the warm season, including flatland, coastland, mountain land, or even the central Tibetan Plateau, displayed similar $\Delta^{200}Hg_D$ and $\Delta^{200}Hg_P$ values of approximately 0.20‰ (Figure 5). Moreover, the average isotope values of both phases in the Great Lakes region were consistent with those in bulk Hg from precipitation collected more than a decade ago.[31,32,36] Aerosol Hg from the Pic du Midi Observatory, Guiyang city, and Xiamen city all presented similar Δ^{200}Hg values of around 0.20‰.[22,23,28] It is generally assumed that the two phases are dominated by different sources, and the aerosol values should be different from those of precipitation. Hence, the observed similarity may suggest that Hg(II) from stratospheric intrusion is not the sole cause for the positive Δ^{200}Hg in atmospheric Hg(II).[11,12] Particularly the Tibetan Plateau, with its high altitude of more than 4000 m a.l.s., should be vulnerable to stratospheric invasion. Nevertheless, the detected Δ^{200}Hg values in year-round precipitation on the Tibetan Plateau (0.16 ± 0.10‰, 2sd, $n = 19$, for Hg_D; 0.16 ± 0.15‰, 2sd, $n = 18$, for Hg_P) were similar to those observed in other regions of the same latitude.[51] Even the maximum Δ^{200}Hg value of 0.28‰ in Tibetan precipitation was much lower compared to that of Peterborough, which suggests no significant stratospheric invasion of atmospheric Hg(II) on the Tibetan Plateau.[51] Due to the high wind speed in the upper troposphere and stratosphere (>50 m/s), the polar vortex got stretched out of shape in the stratosphere and slid southward off the pole. This resulted in a mixing of air masses, equalizing atmospheric Δ^{200}Hg to some degree. In this fashion, the high Δ^{200}Hg of stratospheric Hg(II) could readily diffuse globally through vertical transports (gravitational sedimentation and scavenging by clouds),[49,50] just as observed and modeled in stratosphere−troposphere transport,[52−54] and subsequently enter into the terrestrial ecosystem, causing a slightly positive Δ^{200}Hg in atmospheric Hg(II) (precipitation

https://doi.org/10.1021/acs.est.2c02613
Environ. Sci. Technol. 2022, 56, 12713−12722

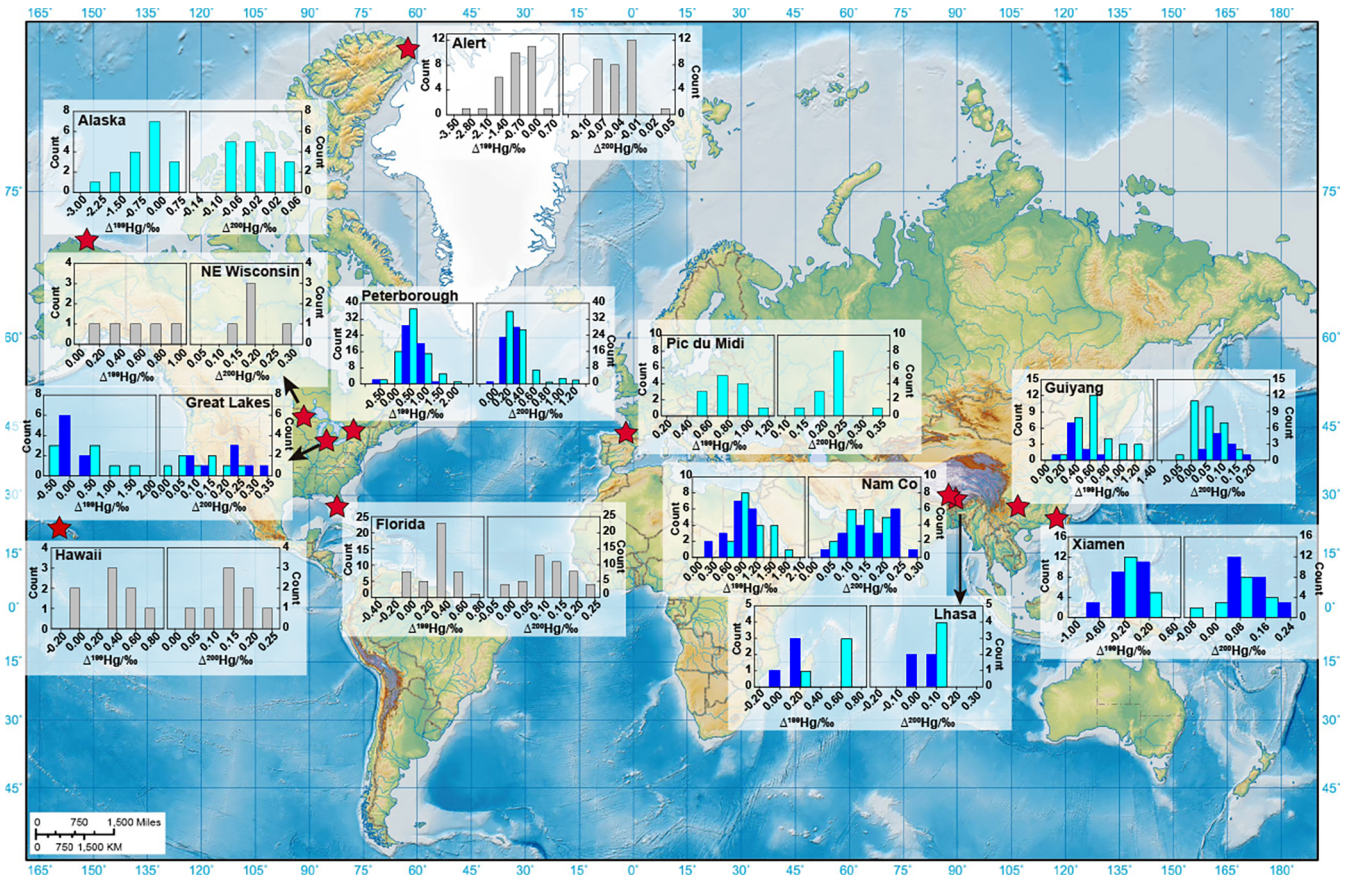

Figure 5. Global distribution of Δ^{199}Hg and Δ^{200}Hg in atmospheric precipitation.[5,22,23,25,28,31,32,36,38,40,41,43,46,47,51]

and aerosols), where no significant stratosphere intrusion (except for polar regions) exists.

Although the Great Lakes region is close to Peterborough and may also experience possible intrusion, the limited numbers of snow samples from five events collected in the winter did not display correspondingly high Δ^{200}Hg values.[32] Meanwhile, the negative Δ^{200}Hg value in Arctic snow is inherited from GEM, when the oxidation is nearly complete,[25] which could exclude oxidation in the ABL as the origin of even-MIF.[28] The negative relationship between Δ^{200}Hg and temperature in this study and a previous study (Figure S3) again emphasized that more precipitation samples must be collected in the winter, especially during periods of stratosphere intrusion (such as Eastern North America), to further validate and define the true mechanisms triggering even-MIF. The apparently negative relationship between Δ^{200}Hg and Δ^{204}Hg, as well as the magnitude of even-MIF in both phases of precipitation Hg compared to other regions, could provide a promising explanation for naturally occurring even-MIF and help to understand the underlying mechanisms triggering even-MIF.

4. ENVIRONMENTAL IMPLICATIONS

Atmospheric precipitation samples collected from Peterborough during cold winter months revealed significant variations in Hg isotopic composition and confirmed again the significant even-Hg isotope anomalies found in 2010. The high magnitude of even-MIF, the apparent negative relationship between Δ^{200}Hg and Δ^{204}Hg, and the negative relationship between Δ^{200}Hg and temperature all contribute to our understanding the underlying mechanisms triggering even-MIF. Inconsistent variations of odd- and even-MIF in sequential precipitation samples events further support the conceptual model that atmospheric Hg(II) with significant even-MIF originated in the stratosphere or tropopause and is transported by the stratosphere polar vortex to regions further south during cold winter months. This provides a promising explanation for naturally occurring even-MIF observations that could originate exclusively from upper tropospheric and/or stratospheric photochemical reactions. Thus, the highly positive Δ^{200}Hg value in precipitation from Peterborough suggests an heterogeneity of atmospheric Δ^{200}Hg and an urgent need for establishing an updated model to constrain the deposition of atmospheric Hg(II) with the aid of atmospheric odd-MIF and even-MIF data.

The horizontal movement of the air mass in the upper troposphere and lower stratosphere may homogenize reactive gaseous mercury (RGM) to some degree. Subsequent vertical mixing would transport Hg(II) downward, which would result in a global atmospheric distribution of positive Δ^{200}Hg originally formed elsewhere. The even-MIF in atmospheric samples is captured particularly in precipitation and may reflect the intensity of local or regional stratosphere-to-troposphere transport processes. It is currently debated that global warming may increase the frequency and/or the intensity of polar stratospheric vortexes, but this warrants further evaluation.[55,56] On the basis of our findings, particularly the negative relationship between Δ^{200}Hg and temperature, the determination of Δ^{200}Hg in atmospheric precipitation may be an alternative and credible indicator of polar vortex and

https://doi.org/10.1021/acs.est.2c02613
Environ. Sci. Technol. 2022, 56, 12713−12722

stratospheric matter intrusion, as has also been suggested for the MIF of sulfur isotopes.[57] We propose that long-term monitoring of even-MIF (Δ^{200}Hg) in atmospheric precipitation could even be an alternative tracer of matter transport from the stratosphere to the troposphere, whereby the Peterborough region just happens to be a very suitable candidate location for monitoring this process.

■ ASSOCIATED CONTENT

Supporting Information

The Supporting Information is available free of charge at https://pubs.acs.org/doi/10.1021/acs.est.2c02613.

Materials and methods (PDF)

Additional figures and a table as described in the text (PDF)

■ AUTHOR INFORMATION

Corresponding Author

Holger Hintelmann − *Chemistry Department, Trent University, Peterborough, Ontario K9J 7B8, Canada*; Email: hhintelmann@trentu.ca

Authors

Shengliu Yuan − *Chemistry Department, Trent University, Peterborough, Ontario K9J 7B8, Canada*; orcid.org/0000-0002-1512-5127

Jiubin Chen − *Institute of Surface-Earth System Science, Tianjin University, Tianjin 300072, People's Republic of China*; orcid.org/0000-0001-7299-0355

Hongming Cai − *Institute of Surface-Earth System Science, Tianjin University, Tianjin 300072, People's Republic of China*

Wei Yuan − *Institute of Surface-Earth System Science, Tianjin University, Tianjin 300072, People's Republic of China*

Sheng He − *Institute of Surface-Earth System Science, Tianjin University, Tianjin 300072, People's Republic of China*

Ke Zhang − *Institute of Surface-Earth System Science, Tianjin University, Tianjin 300072, People's Republic of China*; orcid.org/0000-0003-3582-8839

Yuanyuan Zhang − *Key Laboratory of Environmental Geochemistry, Institute of Geochemistry, Chinese Academy of Sciences, Guiyang, Guizhou 550002, People's Republic of China*

Yulong Liu − *Key Laboratory of Environmental Geochemistry, Institute of Geochemistry, Chinese Academy of Sciences, Guiyang, Guizhou 550002, People's Republic of China*

Complete contact information is available at: https://pubs.acs.org/10.1021/acs.est.2c02613

Notes

The authors declare no competing financial interest.

■ ACKNOWLEDGMENTS

This study was funded by the Natural Science Foundation of China (41625012, 41830647, 41903014) and the Natural Sciences and Engineering Research Council of Canada (RGPIN-2018-05421). The authors acknowledge an associate editor and the anonymous reviewers, who greatly improved the quality of the manuscript.

■ REFERENCES

(1) Spiegel, S. J. New mercury pollution threats: a global health caution. *Lancet* **2017**, *390* (10091), 226−227.

(2) Landrigan, P. J.; Wright, R. O.; Birnbaum, L. S. Mercury Toxicity in Children. *Science* **2013**, *342* (6165), 1447−1447.

(3) Lehnherr, I. Methylmercury biogeochemistry: a review with special reference to Arctic aquatic ecosystems. *Environ. Rev.* **2014**, *22* (3), 229−243.

(4) Amos, H. M.; Jacob, D. J.; Streets, D. G.; Sunderland, E. M. Legacy impacts of all-time anthropogenic emissions on the global mercury cycle. *Global Biogeochem Cy* **2013**, *27* (2), 410−421.

(5) Obrist, D.; Agnan, Y.; Jiskra, M.; Olson, C. L.; Colegrove, D. P.; Hueber, J.; Moore, C. W.; Sonke, J. E.; Helmig, D. Tundra uptake of atmospheric elemental mercury drives Arctic mercury pollution. *Nature* **2017**, *547* (7662), 201−204.

(6) Wang, F.; Outridge, P. M.; Feng, X.; Meng, B.; Heimbürger-Boavida, L.-E.; Mason, R. P. How closely do mercury trends in fish and other aquatic wildlife track those in the atmosphere? − Implications for evaluating the effectiveness of the Minamata Convention. *Sci. Total Environ.* **2019**, *674*, 58−70.

(7) Johnson, K. P.; Blum, J. D.; Keeler, G. J.; Douglas, T. A. Investigation of the deposition and emission of mercury in arctic snow during an atmospheric mercury depletion event. *Journal of Geophysical Research: Atmospheres* **2008**, *113* (D17), D17304.

(8) Holmes, C. D.; Krishnamurthy, N. P.; Caffrey, J. M.; Landing, W. M.; Edgerton, E. S.; Knapp, K. R.; Nair, U. S. Thunderstorms increase mercury wet deposition. *Environ. Sci. Technol.* **2016**, *50*, 9343.

(9) Seo, Y. S.; Han, Y. J.; Choi, H. D.; Holsen, T. M.; Yi, S. M. Characteristics of total mercury (TM) wet deposition: Scavenging of atmospheric mercury species. *Atmos. Environ.* **2012**, *49*, 69−76.

(10) Bergquist, B. A.; Blum, J. D. Mass-Dependent and -Independent Fractionation of Hg Isotopes by Photoreduction in Aquatic Systems. *Science* **2007**, *318* (5849), 417−420.

(11) Chen, J.; Hintelmann, H.; Feng, X.; Dimock, B. Unusual fractionation of both odd and even mercury isotopes in precipitation from Peterborough, ON, Canada. *Geochim Cosmochim Ac* **2012**, *90* (0), 33−46.

(12) Cai, H.; Chen, J. Mass-independent fractionation of even mercury isotopes. *Science Bulletin* **2016**, *61* (2), 116−124.

(13) Chen, J.; Hintelmann, H.; Zheng, W.; Feng, X.; Cai, H.; Wang, Z.; Yuan, S.; Wang, Z. Isotopic evidence for distinct sources of mercury in lake waters and sediments. *Chem. Geol.* **2016**, *426*, 33−44.

(14) Fu, X.; Zhang, H.; Feng, X.; Tan, Q.; Ming, L.; Liu, C.; Zhang, L. Domestic and transboundary sources of atmospheric particulate bound mercury in remote areas of China: evidence from mercury isotopes. *Environ. Sci. Technol.* **2019**, *53* (4), 1947−1957.

(15) Koster van Groos, P. G.; Esser, B. K.; Williams, R. W.; Hunt, J. R. Isotope Effect of Mercury Diffusion in Air. *Environ. Sci. Technol.* **2014**, *48* (1), 227−233.

(16) Estrade, N.; Carignan, J.; Sonke, J. E.; Donard, O. F. X. Mercury isotope fractionation during liquid-vapor evaporation experiments. *Geochim Cosmochim Ac* **2009**, *73* (10), 2693−2711.

(17) Yu, B.; Fu, X.; Yin, R.; Zhang, H.; Wang, X.; Lin, C.-J.; Wu, C.; Zhang, Y.; He, N.; Fu, P.; Wang, Z.; Shang, L.; Sommar, J.; Sonke, J. E.; Maurice, L.; Guinot, B.; Feng, X. Isotopic composition of atmospheric mercury in China: New evidence for source and transformation processes in air and in vegetation. *Environ. Sci. Technol.* **2016**, *50* (17), 9262−9.

(18) Enrico, M.; Le Roux, G.; Marusczak, N.; Heimburger, L.-E.; Claustres, A.; Fu, X.; Sun, R.; Sonke, J. E. Atmospheric mercury transfer to peat bogs dominated by gaseous elemental mercury dry deposition. *Environ. Sci. Technol.* **2016**, *50* (5), 2405.

(19) Blum, J. D.; Sherman, L. S.; Johnson, M. W. Mercury Isotopes in Earth and Environmental Sciences. *Annu. Rev. Earth Pl Sc* **2014**, *42* (1), 249−269.

(20) Zheng, W.; Hintelmann, H. Isotope Fractionation of Mercury during Its Photochemical Reduction by Low-Molecular-Weight Organic Compounds. *J. Phys. Chem. A* **2010**, *114* (12), 4246−4253.

(21) Blum, J. D.; Johnson, M. W. Recent Developments in Mercury Stable Isotope Analysis. *Reviews in Mineralogy and Geochemistry* **2017**, *82* (1), 733.
(22) Huang, S.; Sun, L.; Zhou, T.; Yuan, D.; Du, B.; Sun, X. Natural stable isotopic compositions of mercury in aerosols and wet precipitations around a coal-fired power plant in Xiamen, southeast China. *Atmos. Environ.* **2018**, *173*, 72−80.
(23) Yuan, S.; Chen, J.; Cai, H.; Yuan, W.; Wang, Z.; Huang, Q.; Liu, Y.; Wu, X. Sequential samples reveal significant variation of mercury isotope ratios during single rainfall events. *Sci. Total Environ.* **2018**, *624*, 133−144.
(24) Huang, Q.; Chen, J.; Huang, W.; Fu, P.; Guinot, B.; Feng, X.; Shang, L.; Wang, Z.; Wang, Z.; Yuan, S.; Cai, H.; Wei, L.; Yu, B. Isotopic composition for source identification of mercury in atmospheric fine particles. *Atmos Chem. Phys.* **2016**, *16* (18), 11773−11786.
(25) Zheng, W.; Chandan, P.; Steffen, A.; Stupple, G.; De Vera, J.; Mitchell, C. P. J.; Wania, F.; Bergquist, B. A. Mercury stable isotopes reveal the sources and transformations of atmospheric Hg in the high Arctic. *Appl. Geochem.* **2021**, *131*, 105002.
(26) Jiskra, M.; Sonke, J. E.; Agnan, Y.; Helmig, D.; Obrist, D. Insights from mercury stable isotopes on terrestrial−atmosphere exchange of Hg(0) in the Arctic tundra. *Biogeosciences* **2019**, *16* (20), 4051−4064.
(27) Jiskra, M.; Heimbürger-Boavida, L.-E.; Desgranges, M.-M.; Petrova, M. V.; Dufour, A.; Ferreira-Araujo, B.; Masbou, J.; Chmeleff, J.; Thyssen, M.; Point, D.; Sonke, J. E. Mercury stable isotopes constrain atmospheric sources to the ocean. *Nature* **2021**, *597* (7878), 678−682.
(28) Fu, X.; Jiskra, M.; Yang, X.; Marusczak, N.; Enrico, M.; Chmeleff, J.; Heimbürger-Boavida, L.-E.; Gheusi, F.; Sonke, J. E. Mass-Independent Fractionation of Even and Odd Mercury Isotopes during Atmospheric Mercury Redox Reactions. *Environ. Sci. Technol.* **2021**, *55* (14), 10164−10174.
(29) Yang, S.; Liu, Y. Nuclear volume effects in equilibrium stable isotope fractionations of mercury, thallium and lead. *Sci. Rep-Uk* **2015**, *5*, 12626.
(30) Mead, C.; Lyons, J. R.; Johnson, T. M.; Anbar, A. D. Unique Hg Stable Isotope Signatures of Compact Fluorescent Lamp-Sourced Hg. *Environ. Sci. Technol.* **2013**, *47* (6), 2542−2547.
(31) Gratz, L. E.; Keeler, G. J.; Blum, J. D.; Sherman, L. S. Isotopic Composition and Fractionation of Mercury in Great Lakes Precipitation and Ambient Air. *Environ. Sci. Technol.* **2010**, *44* (20), 7764−7770.
(32) Kurz, A. Y.; Blum, J. D.; Johnson, M. W.; Nadelhoffer, K.; Zak, D. R. Isotopic composition of mercury deposited via snow into mid-latitude ecosystems. *Sci. Total Environ.* **2021**, *784*, 147252.
(33) Putnam, A. E.; Broecker, W. S. Human-induced changes in the distribution of rainfall. *Science Advances* **2017**, *3* (5), e1600871.
(34) Puntsag, T.; Mitchell, M. J.; Campbell, J. L.; Klein, E. S.; Likens, G. E.; Welker, J. M. Arctic Vortex changes alter the sources and isotopic values of precipitation in northeastern US. *Sci. Rep-Uk* **2016**, *6* (1), 22647.
(35) Yamaguchi, M.; Chan, J. C. L.; Moon, I.-J.; Yoshida, K.; Mizuta, R. Global warming changes tropical cyclone translation speed. *Nat. Commun.* **2020**, *11* (1), 47.
(36) Sherman, L. S.; Blum, J. D.; Dvonch, J. T.; Gratz, L. E.; Landis, M. S. The use of Pb, Sr, and Hg isotopes in Great Lakes precipitation as a tool for pollution source attribution. *Sci. Total Environ.* **2015**, *502* (0), 362−374.
(37) Perlinger, J. A.; Urban, N. R.; Giang, A.; Selin, N. E.; Hendricks, A. N.; Zhang, H.; Kumar, A.; Wu, S.; Gagnon, V. S.; Gorman, H. S.; Norman, E. S. Responses of deposition and bioaccumulation in the Great Lakes region to policy and other large-scale drivers of mercury emissions. *Environmental Science: Processes Impacts* **2018**, *20* (1), 195−209.
(38) Wang, Z.; Chen, J.; Feng, X.; Hintelmann, H.; Yuan, S.; Cai, H.; Huang, Q.; Wang, S.; Wang, F. Mass-dependent and mass-independent fractionation of mercury isotopes in precipitation from Guiyang, SW China. *Cr Geosci* **2015**, *347* (7−8), 358−367.
(39) Yuan, W.; Sommar, J.; Lin, C.-J.; Wang, X.; Li, K.; Liu, Y.; Zhang, H.; Lu, Z.; Wu, C.; Feng, X. Stable Isotope Evidence Shows Re-emission of Elemental Mercury Vapor Occurring after Reductive Loss from Foliage. *Environ. Sci. Technol.* **2019**, *53* (2), 651−660.
(40) Sherman, L. S.; Blum, J. D.; Keeler, G. J.; Demers, J. D.; Dvonch, J. T. Investigation of Local Mercury Deposition from a Coal-Fired Power Plant Using Mercury Isotopes. *Environ. Sci. Technol.* **2012**, *46* (1), 382−390.
(41) Demers, J. D.; Sherman, L. S.; Blum, J. D.; Marsik, F. J.; Dvonch, J. T. Coupling atmospheric mercury isotope ratios and meteorology to identify sources of mercury impacting a coastal urban-industrial region near Pensacola, Florida, USA. *Global Biogeochem Cy* **2015**, *29* (10), 1689−1705.
(42) Huang, Q.; He, X.; Huang, W.; Reinfelder, J. R. Mass-Independent Fractionation of Mercury Isotopes during Photo-reduction of Soot Particle Bound Hg(II). *Environ. Sci. Technol.* **2021**, *55*, 13783.
(43) Lepak, R.; Yin, R.; Krabbenhoft, D. P.; Ogorek, J. M.; DeWild, J. F.; Holsen, T. M.; Hurley, J. P. Use of Stable Isotope Signatures to Determine Mercury Sources in the Great Lakes. *Environmental Science & Technology Letters* **2015**, *2*, 335.
(44) Wang, S.; McNamara, S. M.; Moore, C. W.; Obrist, D.; Steffen, A.; Shepson, P. B.; Staebler, R. M.; Raso, A. R. W.; Pratt, K. A. Direct detection of atmospheric atomic bromine leading to mercury and ozone depletion. *Proc. Natl. Acad. Sci. U. S. A.* **2019**, *116*, 201900613.
(45) Douglas, T. A.; Blum, J. D. Mercury isotopes reveal atmospheric gaseous mercury deposition directly to the Arctic coastal snowpack. *Environmental Science & Technology Letters* **2019**, *6* (4), 235−242.
(46) Sherman, L. S.; Blum, J. D.; Johnson, K. P.; Keeler, G. J.; Barres, J. A.; Douglas, T. A. Mass-independent fractionation of mercury isotopes in Arctic snow driven by sunlight. *Nature Geosci* **2010**, *3* (3), 173−177.
(47) Yuan, S.; Zhang, Y.; Chen, J.; Kang, S.; Zhang, J.; Feng, X.; Cai, H.; Wang, Z.; Wang, Z.; Huang, Q. Large Variation of Mercury Isotope Composition During a Single Precipitation Event at Lhasa City, Tibetan Plateau, China. *Procedia Earth and Planetary Science* **2015**, *13*, 282−286.
(48) Porter, T. J.; Schoenemann, S. W.; Davies, L. J.; Steig, E. J.; Bandara, S.; Froese, D. G. Recent summer warming in northwestern Canada exceeds the Holocene thermal maximum. *Nat. Commun.* **2019**, *10* (1), 1631.
(49) Lyman, S. N.; Jaffe, D. A. Formation and fate of oxidized mercury in the upper troposphere and lower stratosphere. *Nature Geosci* **2012**, *5* (2), 114−117.
(50) Slemr, F.; Weigelt, A.; Ebinghaus, R.; Bieser, J.; Brenninkmeijer, C. A. M.; Rauthe-Schöch, A.; Hermann, M.; Martinsson, B. G.; van Velthoven, P.; Bönisch, H.; Neumaier, M.; Zahn, A.; Ziereis, H. Mercury distribution in the upper troposphere and lowermost stratosphere according to measurements by the IAGOS-CARIBIC observatory: 2014−2016. *Atmos. Chem. Phys.* **2018**, *18* (16), 12329−12343.
(51) Yuan, S.; Chen, J.; Sun, R.; Zheng, W.; Cai, H.; Yuan, W.; Meng, M.; Kang, S.; Hintelmann, H., Stable isotopes reveal strong control of monsoon circulation on atmospheric mercury budgets on Tibetan Plateau. Manuscript in preparation.
(52) Abalos, M.; Orbe, C.; Kinnison, D. E.; Plummer, D.; Oman, L. D.; Jöckel, P.; Morgenstern, O.; Garcia, R. R.; Zeng, G.; Stone, K. A.; Dameris, M. Future trends in stratosphere-to-troposphere transport in CCMI models. *Atmos Chem. Phys.* **2020**, *20* (11), 6883−6901.
(53) Kuang, S.; Newchurch, M. J.; Burris, J.; Wang, L.; Knupp, K.; Huang, G. Stratosphere-to-troposphere transport revealed by ground-based lidar and ozonesonde at a midlatitude site. *Journal of Geophysical Research: Atmospheres* **2012**, *117* (D18), 1.
(54) Schmidt, G. A.; Hoffmann, G.; Shindell, D. T.; Hu, Y. Modeling atmospheric stable water isotopes and the potential for constraining

https://doi.org/10.1021/acs.est.2c02613
Environ. Sci. Technol. 2022, 56, 12713−12722

cloud processes and stratosphere-troposphere water exchange. *Journal of Geophysical Research: Atmospheres* **2005**, *110* (D21), 1.
(55) Hu, D.; Guan, Z.; Tian, W.; Ren, R. Recent strengthening of the stratospheric Arctic vortex response to warming in the central North Pacific. *Nat. Commun.* **2018**, *9* (1), 1697.
(56) Zhang, P.; Wu, Y.; Simpson, I. R.; Smith, K. L.; Zhang, X.; De, B.; Callaghan, P. A stratospheric pathway linking a colder Siberia to Barents-Kara Sea sea ice loss. *Science Advances* **2018**, *4* (7), eaat6025.
(57) Lin, M.; Zhang, X.; Li, M.; Xu, Y.; Zhang, Z.; Tao, J.; Su, B.; Liu, L.; Shen, Y.; Thiemens, M. H. Five-S-isotope evidence of two distinct mass-independent sulfur isotope effects and implications for the modern and Archean atmospheres. *Proc. Natl. Acad. Sci. U. S. A.* **2018**, *115*, 8541.

https://doi.org/10.1021/acs.est.2c02613
Environ. Sci. Technol. 2022, 56, 12713−12722